Environmental Science Nano

ROYAL SOCIETY OF CHEMISTRY

PAPER

View Article Online
View Journal | View Issue

Cite this: *Environ. Sci.: Nano*, 2023, **10**, 3039

Matrix-driven environmental fate and effects of silver nanowires during printed paper electronics end of life†

Andrea Carboni, *[ab] Danielle L. Slomberg,[a] Amazigh Ouaksel,[a] Lenka Brousset,[c] Andrea Campos,[d] Bernard Angeletti,[a] Bahareh Zareeipolgardani,[e] Gael Depres,[f] Alain Thiéry,[c] Jerome Rose, [ag] Laurent Charlet [e] and Melanie Auffan [ag]

The release of engineered nanomaterials (ENMs) during manufacturing, use and disposal of nano-enabled products (NEPs) is a potential route of environmental nanopollution. To date, there is limited knowledge on the ecological impact of ENMs incorporated in NEP matrices and how they compare to pristine nanoparticles. Here, we examined the fate and effect of silver nanowires (AgNWs) embedded in a cellulose matrix for the production of printed paper electronics (PPE) (nano)technologies. The fate and impact of fragmented AgNWs-PPE was monitored for 21 days in freshwater mesocosms mimicking a pond ecosystem. The Ag release and AgNWs-PPE behavior in water was further characterized in abiotic batch incubations. Qualitative and quantitative analyses were carried out to estimate the Ag partitioning between the environmental compartments and the aging of AgNWs-PPE as well as bioaccumulation and behavioral responses in biota. In contaminated pond mesocosms, the NEP cellulose/polyvinylidene chloride matrix resulted in rapid settling of the Ag on the sediments and prevented Ag release into the water column. The highest aqueous concentration measured corresponded to less than 0.5% of the total Ag introduced. The AgNWs-PPE fragments accumulated at the water sediment interface, where they were rapidly (bio)degraded and became bioavailable for benthic organisms. Aquatic snails accumulated a significant fraction of the Ag (1.4 ± 0.5%) and displayed enhanced burrowing behavior in comparison to controls. In batch experiments, alteration of the ENM morphology was evident at the NEP surface. Here, the colocalization of Ag and S clusters suggests aging *via* sulfidation, similar to other pristine Ag ENMs. However, the cellulose matrix prevented weathering of the AgNWs within the NEP, which presented a near-pristine state even after 21 days of incubation. Overall, these results indicate that the fate and impact of Ag embedded in the AgNWs-PPE were driven by the cellulose matrix. In particular, given the specific properties and behavior of paper-based (nano)products, these may constitute a unique category when evaluating NEP environmental impact. The data gathered in this study can help in defining the environmental fate of such materials and provide useful information to address future studies focused on ENM environmental fate and risk assessment in a life-cycle perspective.

Received 26th April 2023,
Accepted 31st August 2023

DOI: 10.1039/d3en00263b

rsc.li/es-nano

Environmental significance

The environmental release of engineered nanomaterials (ENMs) may occur during manufacturing, use and disposal of nano-enabled products (NEPs). In this study, we investigated the impact of fragmented printed paper electronics containing silver nanowires on a freshwater ecosystem. Aquatic mesocosm experiments were performed to represent realistic exposure scenarios and NEP aging. The results obtained highlight the role of the paper NEP matrix on both the ENM fate (partitioning, transformation) and effects on biota (bioaccumulation, altered behavior). The data gathered can help in defining the environmental fate of such paper-based NEP materials. Furthermore, they provide useful information to address future studies focused on ENM environmental modelling and regulation as well as fate and risk assessment in a life-cycle perspective.

[a] *CNRS, Aix-Marseille Univ., IRD, INRAE, CEREGE, 13545 Aix-en-Provence, France*
[b] *Dipartimento di Chimica "Giacomo Ciamician", Alma Mater Studiorum-Università di Bologna, Via Francesco Selmi 2, 40126 Bologna, Italy. E-mail: andrea.carboni9@unibo.it*
[c] *CNRS, IRD, IMBE, Aix-Marseille Univ, Avignon Univ., Marseille, France*
[d] *CNRS, Aix Marseille Université, Centrale Marseille, FSCM (FR1739), CP2M, 13397 Marseille, France*
[e] *Université Grenoble Alpes, Université Savoie Mont Blanc, CNRS, IRD, IFSTTAR, ISTerre, Grenoble 38400, France*
[f] *Fedrigoni, 10 Rue Jean Arnaud, 38500 Voiron, France*
[g] *Civil and Environmental Engineering Department, Duke University, Durham, North Carolina 27707, USA*

† Electronic supplementary information (ESI) available. See DOI: https://doi.org/10.1039/d3en00263b

1. Introduction

Nanotechnologies are expected to impact our future with the development of safer and sustainable solutions in the context of environmental and energetic transition.[1] In this framework, green (nano)technologies such as printed paper electronic (PPE) devices are an emerging and potentially game-changing technology due to ease of recycling, economics of manufacture and applicability to flexible electronics.[2] However, the environmental safety and sustainability aspects of nano-enabled products (NEPs) are being investigated at a relatively slow pace compared to their development and commercialization.[3] Recently, silver nanowires (AgNWs) have gathered attention in PPE due to their excellent optoelectronic properties, ease of processing, and large-scale fabrication capability.[4] An expected promising application of AgNW-based PPE is the production of sensors and electric device displays of high transparency, flexibility, and stretchability.[5]

Although AgNW-based PPE can represent a robust, more sustainable and eco-friendly alternative to conventional ones, knowledge on their environmental risk is largely unknown.[2,6] Furthermore, the existing data sets generated from exposure and hazard studies with pristine Ag-based ENMs could not be representative of Ag-based NEP behavior, fate and hazard and are inadequate to support meaningful regulation and assessment tasks.[7] Previous studies on Ag NEPs showed that their environmental fate and impact strongly depend on manufacturing processes (*i.e.* with Ag ENMs applied as surface coating or embedded in the product matrix), the initial ENM load and the Ag speciation.[8–11] The NEP matrix is also an important factor driving ENM fate and was proposed as a main criterion when grouping NEP eco-toxicity during the use phase.[12] Pourzahedi *et al.*[13] performed a life cycle assessment of 15 Ag NEPs (textiles and medical fabrics) and highlighted the role of the matrix, with solid polymeric matrices releasing more silver during washing compared to fibrous materials.

A recent study investigated the fate of AgNWs printed on PPE (AgNWs-PPE) during a pilot-scale recycling process,[14] showing that the released effluents were free from Ag, which was retained in the pulp conserved for recycling. The main aim of the present study was to mimic a chronic contamination of an aquatic ecosystem by AgNWs-PPE to assess, under environmentally relevant conditions, the fate and effects upon release in the environment.

Given the expected long PPE lifetime compared to the experiment duration, a pre-aging protocol was applied. In particular, the AgNWs-PPE samples were fragmented in order to obtain a fragmented product (FP), resulting in an increased surface area at the NEP/ecosystem interface.[15] Mesocosms allow for simulating realistic ecological conditions, and experiments can be designed to study the aging of ENMs while characterizing the associated exposure and hazard.[16–18] In the past years, such experimental systems have been extensively applied for the study of ENM fate[19–22] but to a lesser extent of NEP.[23,24] Using freshwater mesocosms, we first characterized the partitioning of Ag between the environmental compartments. The results obtained with AgNWs-PPE were compared to that with pristine AgNWs in order to identify the potential role of the matrix in determining the Ag partitioning. Complementary mechanistic abiotic batch experiments were used to further characterize the fate of the NEP and incorporated ENMs. Eventually, we also investigated the bioaccumulation into benthic grazers and assessed behavioral markers, which can be sensitive tools at concentrations far below the lethal effect.[25]

This study provides realistic environmental exposure data, which are needed to inform decision-making to mitigate or manage the risks associated to ENMs and NEPs.

2. Materials and methods

2.1. PPE and AgNWs

AgNW suspensions were obtained by diluting a commercial standard (nominal 120 μm AgNW length, 20 g_{Ag} L^{-1} in water; ACS Material, CA, USA) in ultrapure water (UPW; Milli-Q®, Merck, Germany). The AgNWs, characterized by scanning electron microscopy (SEM) coupled to energy-dispersive X-ray (EDX) spectroscopy, displayed an average width of 94.3 ± 8.5 nm and an average length of 13.1 ± 4.3 μm (n = 40) (Fig. 1a).

The AgNWs-PPE samples were received from Arjowiggins (now Fedrigoni Co., Voiron, France) as 210 mm × 297 mm sheets consisting of three distinct layers, namely cellulose, an organic coating and conductive ink. Briefly, a 60 μm thick mixed-cellulose nanofibril (CNF) matrix was coated on one side with a layer of polyvinylidene chloride (PVDC, 5 μm thickness). A conductive ink layer (200–300 nm in thickness) incorporating nanocellulose fibers and the AgNWs was applied on top of the organic coating, resulting in a sheet resistance of approximately 30 Ω sq^{-1} across the samples. The concentration of Ag in the final AgNWs-PPE samples was 1.38 ± 0.07 mg g^{-1}.

For both the mesocosm and the abiotic batch experiments, the original AgNWs-PPE sheet samples were fragmented to mimic the potential physicochemical form at which the NEPs are released in the environment during the use phase. The protocol for fragmentation was optimized from procedures reported in the literature.[12,15,24] First, the PPE samples were cut with a ceramic blade to approximately 2 mm × 2 mm fragments and transferred into 2 ml plastic vials (Eppendorf, Hamburg, Germany). Then, two zirconium marbles were added in each of the vials, which were loaded into a Teflon sample holder and soaked in liquid nitrogen. The frozen samples underwent two 30 s cycles of ball-milling at 30 Hz (Mixer Mill MM 400, Retsch). Liquid nitrogen was poured between the two fragmentation cycles to prevent unfreezing. Finally, sieving at 0.5 mm was performed to remove the largest PPE fragments. The AgNWs-PPE fragment size, assessed with optical microscopy, was 107.2 ± 72.2 μm on average (n = 180). As shown in Fig. 1b, in AgNWs-PPE fragments the ENMs were homogeneously distributed on the

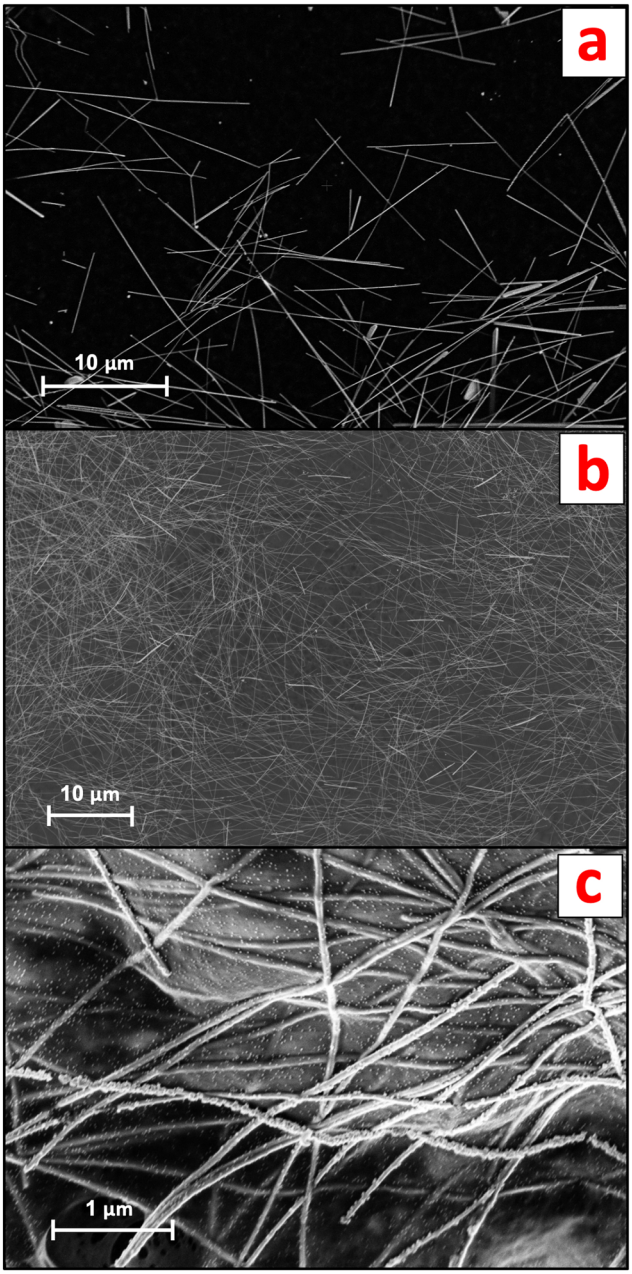

Fig. 1 Scanning electron microscopy analysis of the pristine ENMs and NEPs in this study. (a) The pristine AgNW standard (7 kV, VP BSE detector). (b) The homogeneous surface distribution of AgNWs onto the AgNWs-PPE cellulose matrix (7 kV, VP BSE detector). (c) A close-up of the AgNWs at the AgNWs-PPE surface (0.5 kV, in-lens SE detector).

NEPs and displayed an average diameter of 81.0 ± 11.1 nm and average length of 15.6 ± 3.5 μm (n = 40). At the AgNWs-PPE surface, the AgNWs formed entanglements, displaying protruding nanostructures as well as portions merged within the cellulose matrix (Fig. 1c).

2.2. Mesocosm set-up and operation

Nine indoor aquatic mesocosms were set up to mimic a natural pond ecosystem in the preserved Natura 2000 reserve network, southern France (43.34361°N, 6.259663°E, altitude 107 m.a.s.l., Mediterranean climate). Natural sediments, natural water and organisms were collected at the site within 3 days before setting up the mesocosms. Natural sediments were consecutively sieved at 2 mm and 250 μm to obtain a homogeneous inoculum containing primary producers (*e.g.*, algae, bacteria). Natural water samples were first sieved at 250 μm and then filtered at 0.2 μm to collect suspended matter and biota onto the glass fiber filters. The filters were then placed into 1.5 L Volvic® water under constant agitation for 48 h.

Each mesocosm consisted of a glass tank (750 mm × 200 mm × 600 mm) consecutively filled with a layer of artificial sediment (79% SiO_2, 20% kaolinite, and 1% $CaCO_3$) covered with 300 g of water-saturated natural sediment inoculum (48% water content) and 46 L of Volvic® water, with pH and conductivity values similar to those of the natural pond water. After one week, 0.1 L of water inoculum was added to each aquarium. The mesocosms operated on a 14 h day, 10 h night lighting period. Additional details about mesocosm set-up and monitoring can be found in Auffan *et al.* (2014).[20] The set-up was followed by an equilibration period of two weeks to allow the settling of suspended matter, stabilization of the physicochemical parameters (pH, oxidation–reduction potential [ORP], dissolved O_2) and the development of the primary producers.[26] After the equilibration period, organisms were introduced at a density matching the one observed in the natural biotope. In each mesocosm, 70 mollusks (*A. leucostoma* (Millet 1813), benthic grazers) and 90 micro-crustaceans (*Daphnia* sp., (Muller 1785), planktonic filter feeders) were added. Three days after the addition of the organisms, the mesocosms were randomly assigned to either contaminated or non-contaminated (control) treatments. Contamination was achieved by chronic (press) addition of either fragmented AgNWs-PPE or pristine AgNWs three times per week (9 injections in total) for 21 days. Spiking suspensions were prepared in UPW immediately before addition, vigorously stirred and homogeneously distributed at the water surface. In AgNWs-PPE treatments, each contamination consisted of 175 mg of AgNWs-PPE fragments, corresponding to single Ag doses of 241 μg and a final concentration of 46.7 $\mu g_{Ag}\ L^{-1}$ in the mesocosms. Such a dose was selected as a compromise between the low levels expected in the real ecosystems and the possibility to analyze and characterize the AgNWs-PPE in complex environmental matrices. For AgNW treatments, single Ag doses of 2.42 mg led to a concentration of 470 $\mu g_{Ag}\ L^{-1}$ at the end of the experiment. Such a dose corresponded to an ENM surface-to-mesocosm water ratio of $1.9 \times 10^{-3}\ m^2\ L^{-1}$ (at day 21) and was chosen to match the values recently used for other Ag ENMs in mesocosms.[27]

2.3. Mesocosm sampling and analysis

Several abiotic and biotic parameters were monitored to inform about the exposure and effects of contamination on the aquatic ecosystem. These included the continuous

measurements of water physicochemical properties (pH, oxidation–reduction potential (ORP), electrical conductivity, temperature, and dissolved oxygen) as well as punctual measurements of biotic parameters (Ag concentration in the water column, sediment and organisms, bacterial counting, total organic carbon content (TOC), number of suspended particles and chlorophyll concentration[20,26]).

A first aim of the present study was to quantify the distribution of Ag in the mesocosm following AgNW or AgNWs-PPE contamination. For this purpose, superficial sediments, the water column and the aquatic snails *A. leucostoma* were sampled prior to contamination and then after 7, 14 and 21 days. For water column samples, 10 mL were collected at approximately 10 cm below the water surface, transferred into 15 mL plastic tubes and acidified with 2% ultrapure HNO_3 (Normatom®; SCPScience, Quebec, Canada). Additional 5 mL water samples underwent ultrafiltration at 3 kDa (Amicon Millipore; Merck KgaA, Darmstadt, Germany) prior to analysis for the assessment of dissolved Ag concentrations.

Surficial sediment and *A. leucostoma* samples were dried for 3 days at 65 °C, manually ground in an agate mortar, and then transferred into 15 mL Teflon tubes. 50 mg of each sample was processed as follows. For sediments, 1 mL HCl (34%) (Normatom®), 2 mL HNO_3 (67%) and 0.5 mL HF (47–51%, PlasmaPure®) were added. For *A. leucostoma*, an additional 0.5 mL of H_2O_2 (30–32%, PlasmaPure®) was added. Then, acid digestion was performed at 180 °C in a Milestone UltraWAVE microwave digestion system for 1 h. Metal analysis was performed using an inductively coupled plasma mass spectrometer (ICP-MS, NexIon 300X, Perkin Elmer®).

2.4. Abiotic batch aging experiments

In parallel to the mesocosm experiment, an abiotic batch experiment was carried out for 21 d in 250 mL glass beakers filled with 200 ml Volvic® water to gather mechanistic information on the aging of the AgNWs-PPE fragments under abiotic conditions close to those in the mesocosm (*e.g.* water composition, temperature, day/night cycle). Dosing was carried out with a single addition (pulse dosing) of fragmented AgNWs-PPE at day 0 to match the final dose used in AgNWs-PPE mesocosms (50 μg_{Ag} L^{-1}).

In the abiotic batch experiment the water was sampled similar to the mesocosms for total and dissolved (<3 kDa) Ag concentrations. In addition, at the end of the experiment the AgNWs-PPE were recovered from the beakers, rinsed with UPW and transferred onto glass Petri dishes. The excess water was removed with a pipette and the samples were allowed to dry at room temperature in the dark. The dried samples were stored at 4 °C in the dark for elemental and SEM analyses.

SEM analysis was performed using a Zeiss GeminiSEM 500 ultra-high-resolution field emission electron microscope. For imaging, this system was equipped with a column-mounted detector for high-efficiency surface secondary electron (in-lens SE) detection as well as variable pressure secondary electron (VPSE) and variable pressure backscattered electron (VP BSE) detectors to observe non-conductive samples. The surface analysis of a region of interest was acquired first at low voltage (0.5 kV, in-lens SE detector) to increase topographic contrast and reduce specimen charging, and then at higher energy (7 kV, VP BSE detector) to analyze a deeper fraction of the samples and for energy-dispersive X-ray (EDX) spectroscopy acquisition. The electron acceleration tension was set at 7 kV to achieve sufficient X-ray emission to detect Ag L lines at 3 keV, whereas analysis at higher energies was not possible due to irreversible damage of the PPE matrix. For chemical imaging, EDX was performed using an EDAX Octane silicon drift detector (129 eV energy resolution for manganese). During SEM-EDX mapping, the dwell time for each point was set to 50 μs per pixel and frames were accumulated with drift correction. Reference images taken at the beginning of the acquisition were periodically checked to monitor the potential alteration of the samples during measurements.

3. Results and discussion

3.1. NEP matrix-driven accumulation of Ag on the surficial sediments

In AgNWs-PPE-contaminated mesocosms, the Ag concentration in the sediments increased with time to values significantly higher than those of the controls (Fig. 2a). In detail, following chronic exposure of AgNWs-PPE fragments, the Ag in the sediments was 6.4 ± 1.8 mg kg^{-1} after 7 days and reached 13.8 ± 3.9 mg kg^{-1} at the end of the experiment. These results indicate that the benthic compartment was the main sink for Ag in the simulated pond ecosystem, accumulating up to 97 ± 28% of the total Ag injected at 21 d. The Ag partitioning toward the sediments was accompanied by its minor presence in the water column (Fig. 2b) with a total aqueous concentration of Ag reaching 0.10 ± 0.03 μg L^{-1} after 7 d. This concentration in the water column remained stable until the end of the experiment with 0.19 ± 0.08 μg L^{-1} at 14 d and 0.14 ± 0.01 μg L^{-1} at 21 d, corresponding to approximately 0.5% of the Ag initially introduced. This is in agreement with the macroscopic observation of the fast settling of the AgNWs-PPE fragments right after the injection in the mesocosm surface water. Furthermore, no significant Ag was measured in water after ultrafiltration, indicating either the lack of Ag dissolution or the rapid removal of Ag dissolved species from the water column *via* reprecipitation or complexation, which was already observed in previous studies.[26,28] It must be noted that the Ag species released from the AgNWs-PPE may also be retained by the ultrafiltration membrane applied because of association to the NEP product matrix (*e.g.* Ag–cellulose complexes) or due to absorption into the membrane.

In freshwater mesocosms, important ENM removal from the water column is well known and has been reported for a variety of ecosystem settings and nanomaterials tested.

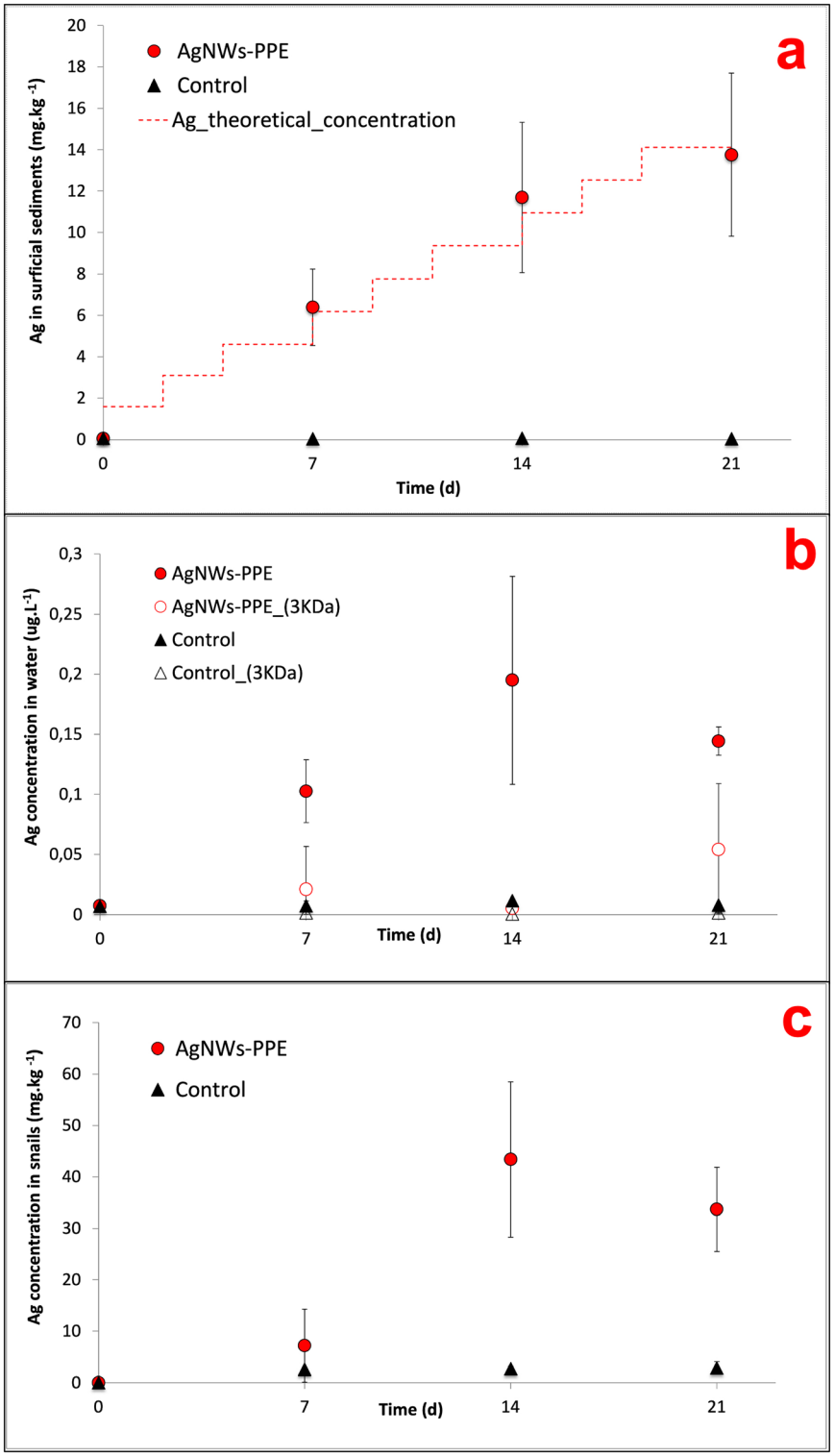

Fig. 2 (a) Total concentration of Ag in the superficial sediments, (b) total and dissolved (<3 kDa) Ag concentrations in the water column, and (c) total concentration of Ag in *A. leucostoma* in mesocosms contaminated with AgNWs-PPE *versus* controls. Dotted line in (a) represents the concentration expected if all the Ag added to the mesocosms settled at the surface of the sediments. Error bars indicate the standard deviation between mesocosms in the same treatment (n = 3).

Previous studies, focused on pristine Ag ENMs with a similar contamination scenario (*i.e.* chronic dosing at similar Ag total doses), reported comparable accumulation in sediment for a range of Ag ENMs differing in coatings and morphology. For instance, in pond indoor mesocosms contaminated with Ag ENM plates, the surficial sediments accumulated 85 ±

19% of the Ag after 28 d of chronic exposure.[21,27] In these cases, compartmentalization into sediments was attributed to ENM homo-aggregation phenomena as well as hetero-aggregation with natural organic matter and suspended solids.[19,26] In this study, AgNWs-PPE fragments were observed to settle rapidly after spiking into the mesocosm surface water, suggesting that the sediment accumulation was likely driven by the cellulose matrix.

Nonetheless, the Ag released in water from the AgNWs-PPE was unexpectedly low for such a surface-coated NEP. Indeed, the silver metal and ENM species release from NEPs is known to rely on the product matrix and manufacturing.[8,11] In general, high release rates can be expected for ENMs present at the surface compared to those incorporated into the NEP bulk.[3,12] For instance, in freshwater aquatic mesocosm studies the Ag released from Ag NEP surface coated textiles displayed higher aqueous concentration and persistence compared to pristine Ag ENMs.[23] In contrast, ENMs included into materials such as acrylic paint displayed diminished release in water.[24] Here, although the AgNWs were present at the surface of the PPE, the Ag partitioning resembled that observed for ENMs incorporated into NEPs such as paint nanocomposite.[24] Such behavior could be due not only to the ecosystem physicochemical properties but also to the low hydrolysis of the cellulose matrix, preventing the short-term Ag release in water as well as the intrinsic physicochemical properties of AgNWs (*e.g.* size, morphology and surface chemistry) that can drive their environmental fate.

To elucidate the role of the PPE matrix in determining the Ag behavior, the Ag partitioning following AgNWs-PPE treatment was compared to that of pristine AgNWs (this study) as well as other pristine Ag nanoplates and nanospheres recently investigated in freshwater mesocosms by our team.[27] For this purpose, the AgNWs were dosed into mesocosms at similar surface area-based concentrations to the ones used for Ag nanoplates and nanospheres (Auffan *et al.*, 2020).[27] As shown in Fig. 3, in mesocosms contaminated with pristine AgNWs, the percentage of injected Ag found in the water column was in the same range of magnitude as those previously observed for Ag nanospheres and nanoplates. The average Ag aqueous fraction of all the pristine Ag ENMs was 9 ± 1% at 14 d and 4 ± 2% on average at 21 d. Hence, for a given surface area-based concentration the Ag release and water persistence are similar between Ag ENMs of different shape and size.

In mesocosms contaminated with AgNWs-PPE, the water Ag fraction was lower than that of pristine Ag ENMs at all the time intervals (0.5 ± 0.2% in average). In particular, when compared to pristine AgNWs, the AgNWs-PPE aqueous Ag was 20-fold lower at 7 d and 6-fold lower at 21 d. These results support the hypothesis that the Ag partitioning observed in AgNWs-PPE treatments was driven by the NEP matrix and not by the specific properties of the AgNWs contained therein.

3.2. Mechanisms of AgNWs-PPE aging in freshwater environments

When assessing the AgNWs-PPE and Ag fate in freshwater mesocosms, a major limitation was due to the impossibility to recover the aged NEP fragments. In particular, the AgNWs-PPE accumulated on the sediment formed flocs, which mixed with and were degraded by the mesocosm's abiotic (mineral sediment matrix) and biotic (biofilm and benthic organisms) components. In order to monitor the AgNWs-PPE transformation and obtain quantitative and qualitative information, we carried out batch experiments under simplified abiotic conditions. Here, the fragmented AgNWs-PPE was incubated under static conditions, similar to the mesocosm experiment with regard to all the abiotic parameters such as water chemistry, irradiation and temperature.

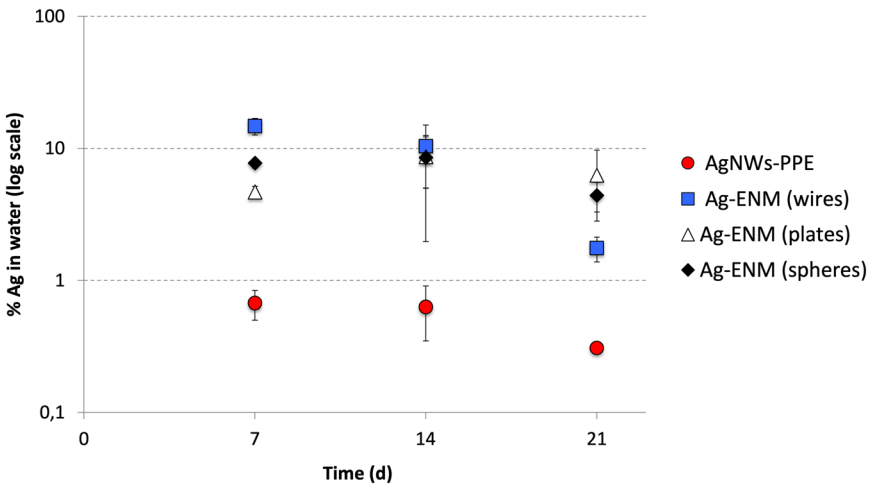

Fig. 3 Comparison between the Ag partitioning in the aqueous phase (% of total Ag introduced) of AgNWs-PPE (red) and pristine AgNWs (wires, blue), Ag nanoplates (plates, white) and Ag nanospheres (spheres, black). Ag nanoplates and Ag nanospheres data were obtained with permission from Auffan *et al.* (2020).[27]

In the batch experiment, the concentrations of Ag in the water increased during the first week and remained stable until the end of the incubation (ESI,† S1). At day 21 the water [Ag] reached 0.93 ± 0.47 μg L^{-1}, which was 5-fold higher than the maximum water concentration measured in the mesocosms. This could be related to the lack of natural suspended matter (*e.g.* organic matter, colloids) and biota (micro- and macro-organisms) in the batch system, which likely plays a role in the removal of dissolved or particulate Ag from the mesocosm water column. At the end of the abiotic incubation, up to 90.6 ± 3.1% of the total Ag was found in the aged NEP fragments recovered and the [Ag] measured after ultrafiltration was negligible, indicating no free Ag ions in solution.

Overall, these results suggest that the Ag remained associated with the NEP matrix and highlight a matrix-driven Ag fate, suggesting that the contamination of aquatic ecosystems with such cellulose/PVDC-based NEPs predominantly involves the exposure to Ag–PPE complexes rather than free ENMs and metal species.

Of course, aging under abiotic conditions was a simplified exposure scenario compared to mesocosms, as it did not account for all biodegradation mechanisms. On the other hand, it allowed for an easier recovery of aged AgNWs-PPE fragments, which were analyzed to gather qualitative information about the distribution, morphology and speciation of the AgNWs in the NEP during aging.

Before aging, the AgNWs were homogeneously distributed onto one side of the NEP (Fig. 1b) where they formed entanglements displaying protruding nanostructures as well as portions merged within the cellulose matrix. Analysis at higher magnification (Fig. 1c) revealed an irregular (non-hexagonal) morphology of the AgNWs as well as the presence of NaCl nanocrystals (approx. 10 nm diameter), confirmed by EDX analysis. The latter could be due to the presence of endogenous Cl species in the samples owing to the PVDC coating.

As shown in Fig. 4, after 21 d of batch incubation, changes in both the NEP matrix and AgNW morphology and distribution were observed. It must be noted that because of the drying process prior to SEM analysis, an alteration of the cellulose matrix and the AgNWs could have occurred. With regard to the ENMs, as shown in Fig. 4a the AgNWs could still be identified on the aged NEP surface but presented extensive breakages and changes in morphology. Furthermore, the AgNWs displayed a lower surface density compared to non-aged NEPs and were all bound to the cellulose matrix, with no protruding nanostructures.

The AgNW density and distribution at the aged surfaces were further investigated by analyzing larger NEP areas. The detection at low energy (focused on the surface) showed that in aged samples, the AgNWs were not homogeneously distributed on the cellulose surface (Fig. 4b). Large areas appeared empty and clusters of nanostructures could only be identified in hotspots. Interestingly, analysis of the same regions at higher energy (both surface and bulk detection) revealed the presence of ENMs incorporated into the cellulose matrix, with distribution similar to that of the original samples (Fig. 4c). These findings suggest that aging of the AgNWs-PPE affected only the AgNWs immediately at

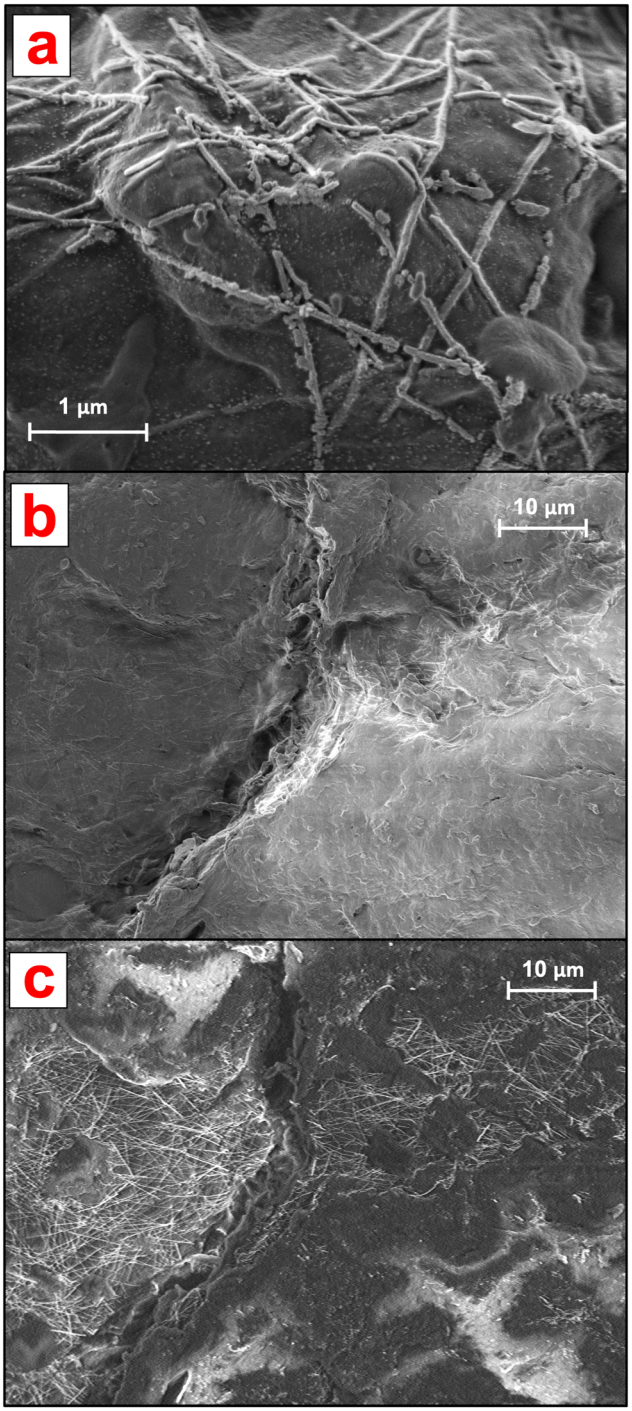

Fig. 4 SEM analysis at the surface of aged AgNWs-PPE samples (21 d abiotic batch incubation). (a) High-magnification image taken at 0.5 keV showing the alteration and fragmentation of the AgNWs at the NEP aged surface. (b) Image of larger AgNWs-PPE fragments area with low voltage acquisition (0.5 kV, in-lens SE detector) showing a limited presence of ENMs at the surface. (c) The image of the same area acquired at higher voltage (7 kV, VP BSE detector) revealed a higher presence of AgNWs in the cellulose matrix bulk.

the NEP surface, thus directly exposed to the outer environment. However, the majority of the ENMs partially or totally incorporated in the matrix, not directly exposed to weathering, presented a near original state. Hence, our hypothesis is that most of the Ag recovered in the cellulose after 21 d of incubation was in the form of ENM, with morphology and distribution resembling those of the original non-aged NEP. In general, these results are in accordance with a recent study on AgNWs-PPE recycling, in which most of the ENMs were retained in the matrix pulp due to embedding by cellulose nanofibrils.[14]

Ag ENMs are known to undergo transformation processes in environmental media, with the formation of novel Ag species (*e.g.* Ag sulfuration, AgCl complexes or precipitates).[10,11,19,27] Understanding the occurrence of such processes in NEPs is fundamental, since they can affect ENM stability, behavior and metal release in aqueous media.[29,30] Here, we collected EDX spectra of the AgNWs at the AgNWs-PPE surface to investigate the potential changes in the chemical composition and silver speciation. As shown in Fig. 5, in aged AgNWs-PPE we observed an important sulfur signal in AgNW hotspots, which was not recorded in the cellulose/PVDC NEP background. Further EDX mapping clarified the colocalization of Ag and S in AgNW hotspots. In freshwater, Ag sulfidation is a major transformation pathway for pristine Ag ENMs. It has been extensively reported in mesocosm studies[19,27] and was linked to a reduced toxicity toward biota.[31,32] It must be noted that sulfidized Ag ENMs are often less soluble than their pristine counterparts, though Ag^+ ion solid diffusion may be high in the Ag_2S surface layer,[33] and their formation in the PPE samples may have enhanced their persistence in the nanoproduct.

The results obtained in the abiotic batch experiment presented here suggest that similar sulfidation processes could also occur when the Ag ENMs are incorporated in NEPs, such as paper-based PPE. However, future studies will need to further characterize these processes under biotic experimental conditions and in the natural environment.

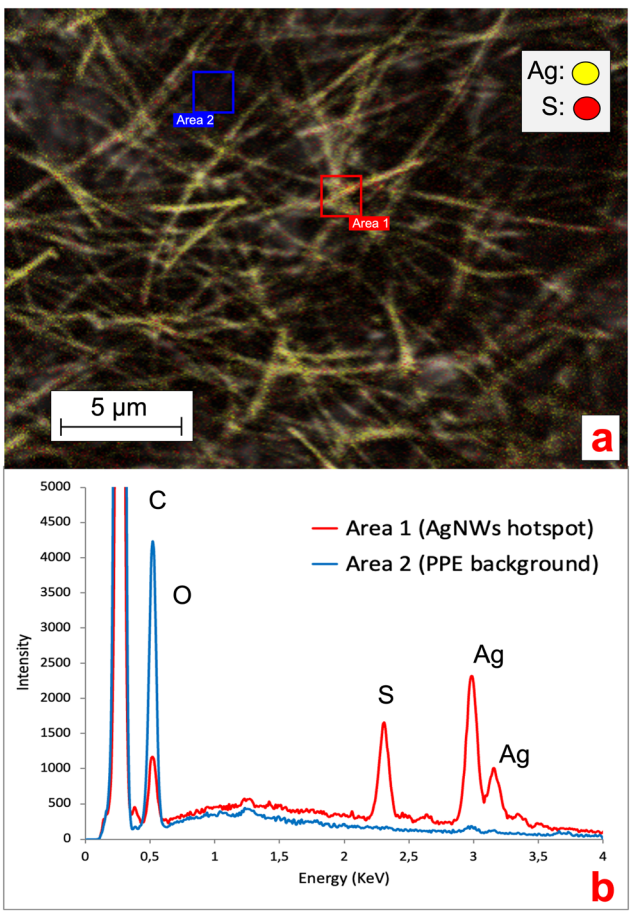

Fig. 5 (a) SEM-EDX mapping at the surface of an aged AgNWs-PPE fragment from batch incubation. Silver and sulfur are represented in yellow and red colors, respectively. (b) EDX spectra of two different locations in the map, namely a AgNW hotspot (area 1, red) and a NEP background (area 2, blue).

3.3. Ecosystem effects induced by AgNW-based PPE

The environmental risk posed by a contaminant depends on its toxicity (hazard), speciation and concentration (exposure) toward target ecological niches.

In the water column of the mesocosms exposed to AgNWs-PPE, chronic contamination did not induce significant effects on most biotic and abiotic parameters. Briefly, no significant changes were observed in pH, redox potential and conductivity following AgNWs-PPE addition. The water TOC was not significantly different, over the course of the incubation, between controls (1.71 ± 0.16 mg L^{-1} on average) and contaminated mesocosms (1.75 ± 0.25 mg L^{-1} on average). The same was valid for chlorophyll and suspended particle amounts as well as planktonic organisms (*Daphnia* sp.) and bacteria populations (ESI,† S2). In general, the low impact on water parameters can be attributed to the Ag speciation and the low Ag water concentration in the mesocosms (Fig. 2b and 5, respectively).

On the other hand, the Ag accumulation in sediments implied a high exposure of the benthic compartment, which was evaluated by monitoring the Ag bioaccumulation and burrowing behavior of the aquatic snail *A. leucostoma*. Herein, Ag concentrations in *A. leucostoma* increased up to 43.4 ± 15.1 mg kg^{-1} (dw) at 14 d and stabilized at 33.7 ± 8.2 mg kg^{-1} at 21 d (Fig. 2c) following AgNWs-PPE treatments. Interestingly, up to 96 ± 5% of the Ag was not leached from the snails after acidic wash of the external bodies, suggesting that the Ag was ingested by the snails and not adsorbed on the shell surface. The stabilization of the Ag concentration taken up by the organism between days 14 and 21 could be due to the combination of both ingestion and depuration processes that are well known in mollusks.[23,34] Such metal uptake/ingestion in benthic organisms has already been reported after contamination with several pristine ENMs such as Ce ENMs,[26] Cu ENMs[24] and Ag ENMs.[23] In the case of NEPs, the Ag bioaccumulation in mud snails exposed in freshwater mesocosms was attributed to a trophic transfer

route from Ag-enriched biofilm.[23] During the present mesocosm experiment, we observed the direct feeding of snails on the AgNWs-PPE fragments accumulated at the sediment/water interface and we hypothesize that the majority of Ag bioaccumulation in snails was due to a direct uptake of AgNWs-PPE. This may have been enhanced by both the cellulose in the NEP matrix, representing a potential food source for the organisms, and the size of fragmented AgNWs-PPE directly bioavailable for the snails. It is noteworthy that the concentrations in the snails observed in this study (~40 mg_{Ag} kg^{-1} at 21 d) were relatively high in consideration of the low dose of total Ag introduced in the mesocosms (~50 μg_{Ag} L^{-1} at 21 d). For instance, similar levels (~100 mg_{Ag} kg^{-1}) were observed in ecotoxicity tests with aquatic snails (*B. glabrata*) exposed to Ag-ENMs at water concentrations up to 50 times higher.[34]

Remarkably, despite significant Ag uptake no enhanced mortality of *A. leucostoma* adults was observed during the experiment, suggesting no acute toxicity of the Ag from aged AgNWs-PPE for the snails. However, the Ag species taken up did not necessarily enter the animal's systemic circulation, and a low toxicity could also be related to sulfidation of the AgNWs at the surface of the aged AgNWs-PPE (Fig. 5), which is known to reduce noxious effects on aquatic biota.[18,31] In addition, no significant effect was observed on benthic bacteria population density (ESI,† S3). However, aquatic organisms can respond to stress with a combination of physiological adaptation and behavioral responses, which are known to occur after heavy metal contamination[35] but are less studied in the case of ENMs and NEPs.[36] In freshwater snails, such traits not only are observed as a response to drought and predation but also result as a consequence of contamination.[37] In the present study, we noticed an increased burrowing of the *A. leucostoma* after one week of chronic contamination and monitored it until the end of the experiment. As shown in Fig. 6, in mesocosms treated with AgNWs-PPE, the snail burrowing activity was observed in up to 50 ± 7% of the snails, on average, during the second week of experiment and 30 ± 10% of the snails, on average, during the third week. This was significantly higher than the controls at days 8, 9 and 15. Similar stress responses in mesocosms contaminated with ENMs were reported by Buffet *et al.*,[36,38] who showed behavioral impairment (burrowing kinetics, feeding rate) of bivalves exposed to Cu and Ag ENMs in seawater ecosystems.

It is worth comparing these biological effects with those observed in the mesocosm contaminated with pristine AgNWs, which will be discussed in detail in a future study. Here, at day 21 the sediments were also the main sink for Ag, accumulating 92 ± 5% of the total dose injected. Furthermore, the Ag concentrations in snails were comparable to those observed in NEP treatments (33 ± 8 mg_{Ag} kg^{-1} for AgNWs-PPE and 69 ± 4 mg_{Ag} kg^{-1} for pristine AgNWs) despite the 10-fold higher total Ag introduced in the mesocosms. However, in the pristine AgNW treatment, no significant burrowing alteration was observed in comparison to controls. These interesting results suggest that the altered behavior following AgNWs-PPE treatments was not due to the absolute amount of Ag uptake. Rather, it could be induced by a different physicochemical state and speciation of the AgNWs in the ingested AgNWs-PPE fragment compared to pristine ENMs, or due to a direct positive effect of the PPE matrix uptake on the mollusk metabolism and behavior. Future studies will need to explore the role of the cellulose matrix in the biodistribution and biotransformation of ENMs in aquatic ecosystems more deeply, *e.g.* by including matrix-only treatments. A better understanding of AgNWs-PPE effects on biota will also require the combination of behavioral trait observations, such as burrowing, with other biological response analysis (*e.g.* biochemical marker analysis).

4. Environmental implications of paper-based NEPs

ENMs are being produced and applied in a wide range of NEPs,[15] where they are incorporated into a variety of liquid

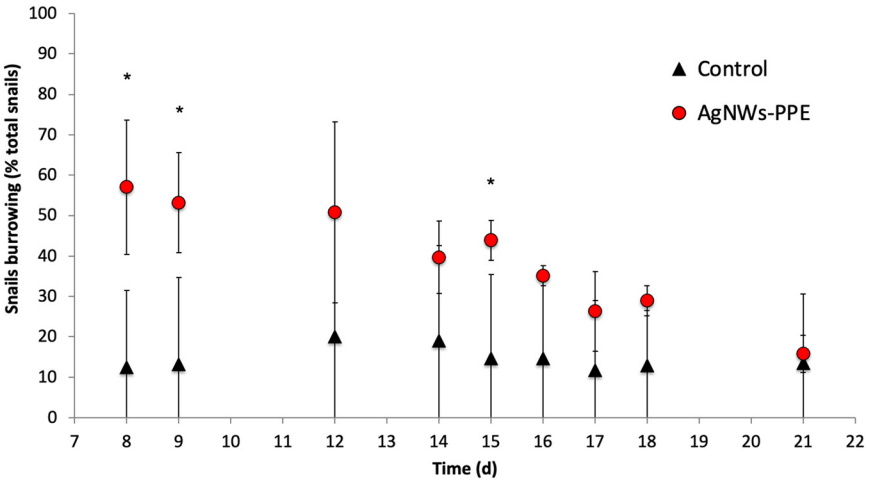

Fig. 6 Percentage of benthic organisms *A. leucostoma* displaying a burrowing trait following exposure to fragmented AgNWs-PPE (red circles) *versus* controls (black triangles). * highlights the differences in mean ± standard deviation (n = 3) between the two treatments.

or solid formulations.[39–41] Several studies recognize that the ENM integration in such matrices determines the properties of the materials that may be released throughout the life cycle.[42] Hence, the matrices can affect the behavior, fate and impact of ENMs when compared to pristine nanoparticles, *e.g.* with regard to their partitioning in the ecosystem, the metal release rates and speciation, and ecotoxicity effects.[12,43] Here, we investigated the fate and effects of AgNWs incorporated into a cellulose/PVDC matrix for the construction of novel AgNWs-PPE nanotechnologies.

In this study, the NEP matrix drove the fate of the incorporated ENMs, influencing their environmental behavior and interaction with biota. In general, the PPE exposure potential (defined as the potential to release ENMs and metals[7]) appeared to be low, and pond ecosystems contaminated with AgNWs-PPE were exposed to ENM–matrix complexes rather than free ENMs and metals. Considering an environmental fate and risk perspective, we observed that the PPE accumulated in the pond sediments, resulting in not only fast removal of Ag from the water column but also an enhanced exposure of the benthic compartment. A lower distribution in water does not necessarily translate to a diminished environmental risk but to a change in the magnitude to which target ecological niches will be exposed. Indeed, a higher accumulation of paper-based NEPs in sediments may imply a higher ENM exposure and bioavailability for benthic organisms, such as the aquatic snails in the present study. Here, no acute toxicity was observed toward the snails at concentrations higher than those expected in real ecosystems.[44] However, paper-based NEPs may represent a food source for aquatic organisms, resulting in an enhanced bioaccumulation and behavioral changes, which must be monitored for a proper assessment of NEP impact and should be explored more thoroughly by future studies.

We also observed that paper-based NEPs represent a very peculiar material whose behavior could be hard to predict compared to other matrices such as plastic or cement nanocomposites.[12] In particular, the fragmented AgNWs-PPE is in principle a (bio)degradable product, but formed flocs that accumulated at the sediment surface under the static mesocosm conditions. Due to the ease of resuspension of such flocs, an enhanced transport may be expected in dynamic lotic environments, such as rivers and flowing water. Future studies will need to address these questions and to further investigate the state at which paper-based NEPs enter and are transformed in the environment as well as their transport and removal from aquatic systems.

Accordingly, when grouping NEP fate and impact based on the matrix material, paper-based NEPs may constitute a category of their own. This is also supported by recent studies testing food contact release of nanoforms from packaging NEPs, which highlighted a different behavior of paper-based NEPs compared to other materials such as polymeric matrices.[45] The data and information reported in this study will be useful for tracking and predicting the fate of ENMs embedded in similar matrices.

Conflicts of interest

There are no conflicts to declare.

Acknowledgements

This work was supported by the Excellence Initiative of Aix-Marseille University – A*MIDEX, a French "Investissements d'Avenir" program, through its associated Labex SERENADE project. This work is also a contribution to the OSU-Institut Pythéas. The authors acknowledge the CNRS funding for the IRP iNOVE.

References

1 J. Rose, M. Auffan, C. de Garidel-Thoron, S. Artous, C. Auplat and G. Brochard, *et al.*, The SERENADE project; a step forward in the safe by design process of nanomaterials: The benefits of a diverse and interdisciplinary approach, *Nano Today*, 2021, **37**, 101065.
2 X. Liao, Z. Zhang, Q. Liao, Q. Liang, Y. Ou and M. Xu, *et al.*, Flexible and printable paper-based strain sensors for wearable and large-area green electronics, *Nanoscale*, 2016, **8**(26), 13025–13032.
3 D. M. Mitrano, S. Motellier, S. Clavaguera and B. Nowack, Review of nanomaterial aging and transformations through the life cycle of nano-enhanced products, *Environ. Int.*, 2015, **77**, 132–147.
4 W. Li, S. Yang and A. Shamim, Screen printing of silver nanowires: balancing conductivity with transparency while maintaining flexibility and stretchability, *npj Flexible Electron.*, 2019, **3**(1), 13.
5 W. Li, E. Yarali, A. Bakytbekov, T. D. Anthopoulos and A. Shamim, Highly transparent and conductive electrodes enabled by scalable printing-and-sintering of silver nanowires, *Nanotechnology*, 2020, **31**(39), 395201.
6 J. Liu, C. Yang, H. Wu, Z. Lin, Z. Zhang and R. Wang, *et al.*, Future paper based printed circuit boards for green electronics: fabrication and life cycle assessment, *Energy Environ. Sci.*, 2014, **7**(11), 3674–3682.
7 P. J. Moeta, J. Wesley-Smith, A. Maity and M. Thwala, Nano-enabled products in South Africa and the assessment of environmental exposure potential for engineered nanomaterials, *SN Appl. Sci.*, 2019, **1**(6), 577.
8 T. M. Benn and P. Westerhoff, Nanoparticle Silver Released into Water from Commercially Available Sock Fabrics, *Environ. Sci. Technol.*, 2008, **42**(11), 4133–4139.
9 L. Geranio, M. Heuberger and B. Nowack, The Behavior of Silver Nanotextiles during Washing, *Environ. Sci. Technol.*, 2009, **43**(21), 8113–8118.
10 C. Lorenz, L. Windler, N. von Goetz, R. P. Lehmann, M. Schuppler and K. Hungerbühler, *et al.*, Characterization of silver release from commercially available functional (nano) textiles, *Chemosphere*, 2012, **89**(7), 817–824.
11 E. Lombi, E. Donner, K. G. Scheckel, R. Sekine, C. Lorenz and N. V. Goetz, *et al.*, Silver speciation and release in

commercial antimicrobial textiles as influenced by washing, *Chemosphere*, 2014, **111**, 352–358.

12 M. J. B. Amorim, S. Lin, K. Schlich, J. M. Navas, A. Brunelli and N. Neubauer, *et al.*, Environmental Impacts by Fragments Released from Nanoenabled Products: A Multiassay, Multimaterial Exploration by the SUN Approach, *Environ. Sci. Technol.*, 2018, **52**(3), 1514–1524.

13 L. Pourzahedi, M. Vance and M. J. Eckelman, Life Cycle Assessment and Release Studies for 15 Nanosilver-Enabled Consumer Products: Investigating Hotspots and Patterns of Contribution, *Environ. Sci. Technol.*, 2017, **51**(12), 7148–7158.

14 B. Zareeipolgardani, A. Piednoir, B. Joyard-Pitiot, G. Depres, L. Charlet and J. Colombani, Multiscale investigation of the fate of silver during printed paper electronics recycling, *Compos. Interfaces*, 2022, 1–14.

15 B. Nowack, A. Boldrin, A. Caballero, S. F. Hansen, F. Gottschalk and L. Heggelund, *et al.*, Meeting the Needs for Released Nanomaterials Required for Further Testing—The SUN Approach, *Environ. Sci. Technol.*, 2016, **50**(6), 2747–2753.

16 A. Masion, M. Auffan and J. Rose, Monitoring the Environmental Aging of Nanomaterials: An Opportunity for Mesocosm Testing?, *Materials*, 2019, **12**(15), 2447.

17 M. Auffan, A. Masion, C. Mouneyrac, C. de Garidel-Thoron, C. O. Hendren and A. Thiery, *et al.*, Contribution of mesocosm testing to a single-step and exposure-driven environmental risk assessment of engineered nanomaterials, *NanoImpact*, 2019, **13**, 66–69.

18 A. Carboni, D. L. Slomberg, M. Nassar, C. Santaella, A. Masion and J. Rose, *et al.*, Aquatic Mesocosm Strategies for the Environmental Fate and Risk Assessment of Engineered Nanomaterials, *Environ. Sci. Technol.*, 2021, **55**(24), 16270–16282.

19 G. V. Lowry, B. P. Espinasse, A. R. Badireddy, C. J. Richardson, B. C. Reinsch and L. D. Bryant, *et al.*, Long-Term Transformation and Fate of Manufactured Ag Nanoparticles in a Simulated Large Scale Freshwater Emergent Wetland, *Environ. Sci. Technol.*, 2012, **46**(13), 7027–7036.

20 M. Auffan, M. Tella, C. Santaella, L. Brousset, C. Paillès and M. Barakat, *et al.*, An adaptable mesocosm platform for performing integrated assessments of nanomaterial risk in complex environmental systems, *Sci. Rep.*, 2014, **4**(1), 5608.

21 B. P. Colman, L. F. Baker, R. S. King, C. W. Matson, J. M. Unrine and S. M. Marinakos, *et al.*, Dosing, Not the Dose: Comparing Chronic and Pulsed Silver Nanoparticle Exposures, *Environ. Sci. Technol.*, 2018, **52**(17), 10048–10056.

22 A. Avellan, M. Simonin, E. McGivney, N. Bossa, E. Spielman-Sun and J. D. Rocca, *et al.*, Gold nanoparticle biodissolution by a freshwater macrophyte and its associated microbiome, *Nat. Nanotechnol.*, 2018, **13**(11), 1072–1077.

23 D. Cleveland, S. E. Long, P. L. Pennington, E. Cooper, M. H. Fulton and G. I. Scott, *et al.*, Pilot estuarine mesocosm study on the environmental fate of Silver nanomaterials leached from consumer products, *Sci. Total Environ.*, 2012, **421–422**, 267–272.

24 M. Auffan, W. Liu, L. Brousset, L. Scifo, A. Pariat and M. Sanles, *et al.*, Environmental exposure of a simulated pond ecosystem to a CuO nanoparticle-based wood stain throughout its life cycle, *Environ. Sci.: Nano*, 2018, **5**(11), 2579–2589.

25 C. Amiard-Triquet, Behavioral Disturbances: The Missing Link between Sub-Organismal and Supra-Organismal Responses to Stress? Prospects Based on Aquatic Research, *Hum. Ecol. Risk Assess.*, 2009, **15**(1), 87–110.

26 M. Tella, M. Auffan, L. Brousset, J. Issartel, I. Kieffer and C. Pailles, *et al.*, Transfer, Transformation, and Impacts of Ceria Nanomaterials in Aquatic Mesocosms Simulating a Pond Ecosystem, *Environ. Sci. Technol.*, 2014, **48**(16), 9004–9013.

27 M. Auffan, C. Santaella, L. Brousset, M. Tella, E. Morel and P. Ortet, *et al.*, The shape and speciation of Ag nanoparticles drive their impacts on organisms in a lotic ecosystem, *Environ. Sci.: Nano*, 2020, **7**(10), 3167–3177.

28 L. M. Furtado, M. E. Hoque, D. M. Mitrano, J. F. Ranville, B. Cheever and P. C. Frost, *et al.*, The persistence and transformation of silver nanoparticles in littoral lake mesocosms monitored using various analytical techniques, *Environ. Chem.*, 2014, **11**(4), 419.

29 G. V. Lowry, K. B. Gregory, S. C. Apte and J. R. Lead, Transformations of Nanomaterials in the Environment, *Environ. Sci. Technol.*, 2012, **46**(13), 6893–6899.

30 J. R. Lead, G. E. Batley, P. J. J. Alvarez, M. N. Croteau, R. D. Handy and M. J. McLaughlin, *et al.*, Nanomaterials in the environment: Behavior, fate, bioavailability, and effects-An updated review: Nanomaterials in the environment, *Environ. Toxicol. Chem.*, 2018, **37**(8), 2029–2063.

31 L. Yuan, C. J. Richardson, M. Ho, C. W. Willis, B. P. Colman and M. R. Wiesner, Stress Responses of Aquatic Plants to Silver Nanoparticles, *Environ. Sci. Technol.*, 2018, **52**(5), 2558–2565.

32 S. G. Lehmann, D. Toybou, A. E. Pradas del Real, D. Arndt, A. Tagmount and M. Viau, *et al.*, Crumpling of silver nanowires by endolysosomes strongly reduces toxicity, *Proc. Natl. Acad. Sci. U. S. A.*, 2019, **116**(30), 14893–14898.

33 P. Simonnin, M. Sassi, B. Gilbert, L. Charlet and K. M. Rosso, Phase Transition and Liquid-like Superionic Conduction in Ag_2S, *J. Phys. Chem. C*, 2020, **124**(18), 10150–10158.

34 E. Oliveira-Filho, D. Muniz, E. Carvalho, P. Cáceres-Velez, M. Fascineli and R. Azevedo, *et al.*, Effects of AgNPs on the Snail Biomphalaria glabrata: Survival, Reproduction and Silver Accumulation, *Toxics*, 2019, **7**(1), 12.

35 J. R. McInnes and F. P. Thurberg, Effects of metals on the behaviour and oxygen consumption of the mud snail, *Mar. Pollut. Bull.*, 1973, **4**, 185–187.

36 P. E. Buffet, O. F. Tankoua, J. F. Pan, D. Berhanu, C. Herrenknecht and L. Poirier, *et al.*, Behavioural and biochemical responses of two marine invertebrates Scrobicularia plana and Hediste diversicolor to copper oxide nanoparticles, *Chemosphere*, 2011, **84**(1), 166–174.

37 P. D. Hazelton, B. Du, S. P. Haddad, A. K. Fritts, C. K. Chambliss and B. W. Brooks, *et al.*, Chronic

fluoxetine exposure alters movement and burrowing in adult freshwater mussels, *Aquat. Toxicol.*, 2014, **151**, 27–35.

38 P. E. Buffet, J. F. Pan, L. Poirier, C. Amiard-Triquet, J. C. Amiard and P. Gaudin, *et al.*, Biochemical and behavioural responses of the endobenthic bivalve Scrobicularia plana to silver nanoparticles in seawater and microalgal food, *Ecotoxicol. Environ. Saf.*, 2013, **89**, 117–124.

39 C. Botta, J. Labille, M. Auffan, D. Borschneck, H. Miche and M. Cabie, *et al.*, TiO2-based nanoparticles released in water from commercialized sunscreens in a life-cycle perspective: Structures and quantities, *Environ. Pollut.*, 2011, **159**(6), 543–1550.

40 N. Bossa, P. Chaurand, C. Levard, D. Borschneck, H. Miche and J. Vicente, *et al.*, Environmental exposure to TiO2 nanomaterials incorporated in building material, *Environ. Pollut.*, 2017, **220**, 1160–1170.

41 L. Scifo, P. Chaurand, N. Bossa, A. Avellan, M. Auffan and A. Masion, *et al.*, Non-linear release dynamics for a CeO2 nanomaterial embedded in a protective wood stain, due to matrix photo-degradation, *Environ. Pollut.*, 2018, **241**, 182–193.

42 S. Liu and T. Xia, Continued Efforts on Nanomaterial-Environmental Health and Safety Is Critical to Maintain Sustainable Growth of Nanoindustry, *Small*, 2020, **16**(21), 2000603.

43 W. Wohlleben, B. Hellack, C. Nickel, M. Herrchen, K. Hund-Rinke and K. Kettler, *et al.*, The nanoGRAVUR framework to group (nano)materials for their occupational, consumer, environmental risks based on a harmonized set of material properties, applied to 34 case studies, *Nanoscale*, 2019, **11**(38), 17637–17654.

44 B. Giese, F. Klaessig, B. Park, R. Kaegi, M. Steinfeldt and H. Wigger, *et al.*, Risks, Release and Concentrations of Engineered Nanomaterial in the Environment, *Sci. Rep.*, 2018, **8**(1), 1565.

45 E. Ruggiero, K. Y. Santizo, M. Persson, C. Delpivo and W. Wohlleben, Food contact of paper and plastic products containing SiO2, Cu-Phthalocyanine, Fe2O3, CaCO3: Ranking factors that control the similarity of form and rate of release, *NanoImpact*, 2022, **25**, 100372.

